

Labelling plants in the Chernobyl way: A new ^{137}Cs and ^{14}C foliar application approach to investigate rhizodeposition and biopore reuse

Callum C. Banfield · Mohsen Zarebanadkouki ·
Bernd Kopka · Yakov Kuzyakov

Received: 3 November 2016 / Accepted: 16 April 2017 / Published online: 4 May 2017
© Springer International Publishing Switzerland 2017

Abstract

Background and aims Biopores as microbial hotspots provide additional nutrients to crops – but only if their roots grow within the biopores. Such reuse has never been quantified as pre-crop-specific biopores are hardly differentiated from the multitude of pre-existing biopores. Quantification requires e.g. radionuclide labelling of pre-crops (^{137}Cs , to label their biopores) and main crops (^{14}C , to detect new roots). Preliminary testing was performed on simulated biopore reuse: both

nuclides given to the same plant were excreted into the same rhizosphere.

Methods *Cichorium intybus* (cv. Puna) and *Medicago sativa* (cv. Planet) were each sequentially labelled via the leaves with ^{137}Cs and $^{14}\text{CO}_2$. β -signals were visualised by imaging of horizontal soil cuts - with and without shielding off the weaker ^{14}C .

Results Both species allocated 7.1–9.4% of the ^{137}Cs and 21–63% of the ^{14}C below ground. The first image gave both activities; while the second gave only ^{137}Cs . Subtracting the second from the first image gave the ^{14}C distribution, resulting in successful separation of the signals. Thus, separate spatial representations of the roots were obtained. Main root locations by ^{137}Cs and ^{14}C showed a very high spatial overlap coefficient (> 0.95).

Conclusions Biopore reuse quantification likely becomes feasible with this sequential labelling and shielding approach.

Responsible Editor: Eric Paterson.

Electronic supplementary material The online version of this article (doi:10.1007/s11104-017-3260-7) contains supplementary material, which is available to authorized users.

C. C. Banfield (✉) · Y. Kuzyakov
Institute for Soil Science of Temperate Ecosystems,
Georg-August-University of Goettingen, Buesgenweg 2,
37077 Goettingen, Germany
e-mail: callumba@gmail.com

M. Zarebanadkouki
Division of Soil Hydrology, Georg-August-University of
Goettingen, Buesgenweg 2, 37077 Goettingen, Germany

B. Kopka
Laboratory for Radioisotopes, Faculty of Forest Sciences and
Forest Ecology, Georg-August-University of Goettingen,
Buesgenweg 2, 37077 Goettingen, Germany

Y. Kuzyakov
Department of Agricultural Soil Science,
Georg-August-University of Goettingen, Buesgenweg 2,
37077 Goettingen, Germany

Keywords Crop rotation · Detritusphere · Foliar application · Leaf feeding · Radionuclides · Root channel · Root system

Introduction

The root system and its surrounding soil, known as the rhizosphere (Hiltner 1904), are recognised as key interfaces of carbon (C) cycling. Roots induce strong chemical, biological and physical changes in soil, e.g. by exudation of easily available carbon sources, i.e.

rhizodeposition. As the exuded C sources boost microorganisms, the rhizosphere is deemed a microbial hot spot (Jones et al. 2009; Kuzyakov and Blagodatskaya 2015; Paterson 2003). After their death, roots leave behind voids, so-called biopores (Kautz et al. 2013), through which subsequently grown crop roots grow faster into the subsoil and reach additional resources. One of the presumably largest benefits for subsequent crops is the biochemical environment created by root decay and rhizodeposition. In the field, even two years after root death and decomposition, C contents in root biopores, also known as the detritosphere, were still 2.5 times higher than in bulk soil, leading to up to 5.5 times higher microbial biomass and concomitantly increased enzyme activities (Hoang et al. 2016; Banfield et al. 2017). This likely causes faster C turnover and simultaneously nutrient mobilisation from soil organic matter and solid phases. Biopores appear particularly interesting for promoting plant growth in low-input systems such as organic agriculture. It was reported that crops growing in previously established biopores may benefit from nutrients and from the reduced mechanical resistance (Athmann et al. 2013; Ehlers et al. 1983; Yunusa and Newton 2003). If biopores are indeed largely beneficial, their relevance depends on if they are reused in a crop rotation or not. Reuse of biopores could be promoted by management practices such as no-till and crop rotations with tap-rooted pre-crops, which create large-sized biopores (Kautz et al. 2013). On the contrary, it is also possible that depending on soil conditions or other not well-understood factors, this may not always be the case: roots may end up trapped within biopores, which may have had their walls compacted due to root expansion or earthworm burrowing (Hirth et al. 2005). Biopores may be lined with hydrophobic root-derived substances hampering water and nutrient uptake (Carminati 2013). What is more, in some biopores the root-soil contact may be limited (White and Kirkegaard 2010). Such points underline that we are far from a full understanding of biopore dynamics and their controlling factors.

Regardless of the positive or negative effects, biopores are re-used by subsequent crops (White and Kirkegaard 2010): barley modified its root size distribution depending on the pre-crop root system (Han et al. 2016). Up to now, there has been only scarce quantitative information on the reuse of biopores by subsequently grown crops. This is due to the challenging and often

impossible determination of roots growing in specific biopores among countless other biopores of varying age and genesis (Athmann et al. 2013; Han et al. 2015). Therefore, a tool is needed to separate and to quantify biopores and active roots. For this purpose, we propose radionuclide labelling of pre-crops with radiocaesium (^{137}Cs), labelling main crops with $^{14}\text{CO}_2$ and visualisation of each. ^{137}Cs was released into the atmosphere by nuclear weapon tests until 1953 and by nuclear power plant accidents, e.g. in Chernobyl, Ukraine (UNSCEAR 2011). ^{137}Cs has been used as a long-term soil erosion proxy all around the globe due to its half-life of ~30 years and its strong binding to soil particles, especially clay (Cremers et al. 1988; Schuller et al. 2002; Walling and He 1999). The Chernobyl fallout including ^{137}Cs has also been used to assess the age of preferential flow paths in soil (Hagedorn and Bundt 2002). This makes ^{137}Cs an excellent candidate for the biopore labelling. Its chemical behaviour is also similar to potassium, which means ^{137}Cs may be used to simulate solute dynamics once released by the roots.

The inspiration for our concept was the path of the ^{137}Cs fallout caused by the Chernobyl nuclear disaster through the plant leaves to the roots and into the rhizosphere, where ^{137}Cs strongly binds to the soil matrix. Our approach imitates this by labelling crops through the leaves with $^{137}\text{CsCl}$ to create ^{137}Cs -labelled roots. The roots may be left to decompose to form ^{137}Cs -labelled biopores before the next crop. The second labelling with ^{14}C is thought to be performed on the new crops. Assimilated $^{14}\text{CO}_2$ will be exuded as ^{14}C -photosynthates into the rhizosphere of some of the previously created ^{137}Cs -biopores. Both radionuclides' β^- decay can be visualised by phosphor imaging of soil cross sections, but the main challenge lies in separating the ^{137}Cs and ^{14}C signals, which are spatially overlapping in some biopores in the case of reuse. The separation of activities should be possible because during the ^{137}Cs decay 95% of the energy is released as β^- radiation with an energy of 514 keV, whereas the maximum energy of the ^{14}C β^- decay is 156 keV (Nucleonica 2014). Therefore, the two β^- radiations can be separated by shielding off the weaker ^{14}C β^- radiation while allowing the higher energy ^{137}Cs radiation to pass through (Amato and Lizio 2009).

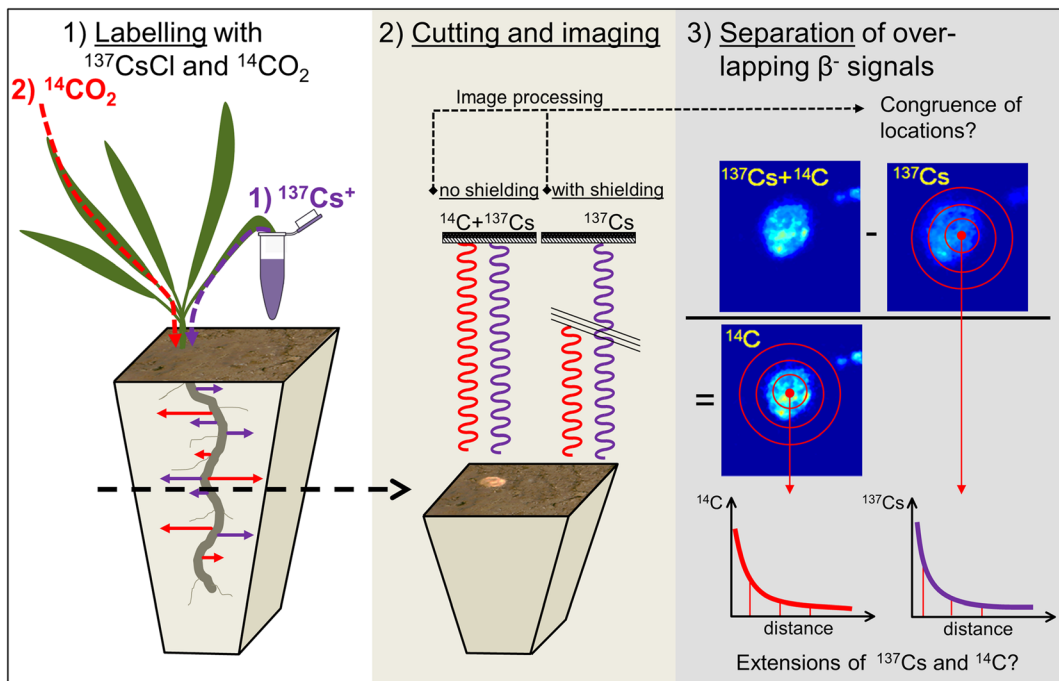


Fig. 1 Concept of the experiment: 1) Labelling the same plants with first ^{137}Cs and then with ^{14}C , 2) imaging with and without shielding and 3) subtracting the signals and image processing

This up-to-now theoretical concept requires at least 1.5 years to test, so we simulated the biopore reuse in a pot experiment to test its feasibility (Fig. 1). The same plants of either fibrous (alfalfa) or tap-rooted (chicory) root system were labelled first with ^{137}Cs through leaf feeding and after a few days with ^{14}C in a $^{14}\text{CO}_2$ atmosphere, instead of waiting for root decomposition and growth of new plants. As both radionuclides are excreted into the same locations, this would be the simulation of a reused biopore, i.e. the spatial overlap of both radionuclides in a specific root channel. Two sequential imagings of soil cross sections with and without shielding and image processing will separate the β^- signals (Fig. 1). Thus, two-dimensional representations of the root systems will be acquired, which can be quantified, and the feasibility of visualising biopore reuse will be apparent.

Material and methods

Soil and plant preparation

Five specimens of chicory (*Cichorium intybus* L. cv. Puna) and five specimens of alfalfa (*Medicago*

sativa L. cv. Planet) were grown for 200 days in pots of 15.5 cm height and 5 cm diameter. These species were chosen, as they feature different root system architectures and both species have been widely used in our research group, i.e. their features and peculiarities are well known. The soil was taken from a long-term field experiment site of the Department of Soil Science of Temperate Ecosystems of the Georg-August - University of Göttingen in Hohenpoelz (Bavaria), Germany. This loamy Luvisol was chosen as its properties are well known through previous studies (Dippold and Kuzyakov 2016; Gunina et al. 2014). Selected soil properties are given in Online Resource 6. The soil was dried at 40 °C, disaggregated by passing through a 2 mm sieve and then mixed with 25% fine sand to reduce shrinking and swelling.

The seeds were germinated on wet filter paper for two days. One seedling was planted in each pot at the depth of 0.5 cm. Plants were kept in controlled conditions, i.e. at a temperature of 22 °C, humidity of 50–60% and constant light intensity of $\sim 200 \mu\text{mol m}^{-2} \text{s}^{-1}$. During the growth period, weak fertilisation was carried out

twice (N_{org} , P_{org} , K) and plants were watered every other day.

Dual labelling experiment

When plants were 200 days old, the labelling experiment started. The ^{137}Cs labelling solution was prepared as follows: 18.5 MBq of $^{137}\text{CsCl}$ dissolved in 0.1 M HCl were obtained from POLATOM (Otwock, Poland) through Hartmann Analytic (Brunswick, Germany). About 50 Bq μl^{-1} were added to aqueous solutions of unlabelled $^{133}\text{CsCl}$ (0.5 mM) (Sigma-Aldrich Chemie GmbH, Munich, Germany) in 5 ml Eppendorf vials (Eppendorf AG, Hamburg, Germany).

For the ^{137}Cs labelling, two chicory leaves of each plant were cut with a razor blade at their widest part and immediately immersed in a 5 ml vial containing 2500 μl of the ^{137}Cs solution (Online Resource 1), whereas 2–3 alfalfa stems were cut with a razor blade and immersed in a 1 ml vial filled with 500 μl ^{137}Cs solution. Both solutions contained the same ^{137}Cs activity concentration of 50 Bq μl^{-1} . It was chosen as previous tests carried out with younger plants with 25 Bq μl^{-1} resulted in satisfying images. Eppendorf vials were put into 20 ml scintillation vials for stability and these in turn fixed by clamps attached to a lab stand (Online Resource 1). Transparent tape was used to secure the plant parts onto the vials and to limit evaporation. To monitor evaporation, one vial was filled with a defined volume of $^{133}\text{CsCl}$ solution and left next to the plants. There were considerable differences in the volumes of solution taken up by the plants. As the alfalfa vials were empty after 24 h, 250 μl of distilled water was added to enable uptake of residual activity possibly remaining in the vials. Chicory leaves took up less solution, so that after 2 days the immersed leaves were taken out of the vial, patted dry and two different leaves were cut and immersed for another 24 h. Remaining ^{137}Cs activity in the vials was determined by the HiDex Automatic Gamma counter (550–750 keV, 3" NaI detector, count time 10 min, count efficiency 17.5%; HiDex Oy, Turku, Finland). In this case, the γ radiation from the ^{137}Cs decay chain is used instead of the direct ^{137}Cs β^- emission. The remaining activities in the vials were related to the

initial activities to calculate the uptake of the ^{137}Cs tracer.

$$Eff_{137\text{Cs}} = \frac{(A_{\text{initial}} - A_{\text{vial}})}{A_{\text{initial}}} \times 100\% \quad (1)$$

with:

- $Eff_{137\text{Cs}}$ the uptake efficiency of the ^{137}Cs tracer from the vial [%]
- A_{vial} the ^{137}Cs activity of the vial and its remaining volume after labelling [Bq]
- A_{initial} the ^{137}Cs activity of the vial and the tracer solution prior to labelling [Bq]

To show the potential of the approach, the same plants were labelled also with $^{14}\text{CO}_2$ instead of waiting for root decomposition and growth of new plants (Fig. 1). $^{14}\text{CO}_2$ labelling was performed in an airtight and transparent plastic chamber under a plant growth lamp. 5 MBq of $\text{Na}_2^{14}\text{CO}_3$ (Hartmann Analytic, Brunswick, Germany) were dissolved by phosphoric acid (Sigma-Aldrich Chemie GmbH, Munich, Germany) and the formed $^{14}\text{CO}_2$ was pumped into the chamber by a peristaltic pump and cycled for 36 h. A 120-mm fan supported the even distribution of the $^{14}\text{CO}_2$ inside the chamber. Four days after the ^{14}C labelling, the soil cores were cut horizontally at the depth of 5 cm below the soil surface with a sharp utility knife. Prior to this, the plastic pot was cut open with a cut-off wheel tool (Dremel 4000 series, Dremel Corp. Racine, WI, U.S.A.).

^{137}Cs and ^{14}C imaging

The cut soil surfaces were placed on phosphor imaging plates (BAS-MS 2040; 20 by 40 cm; Fujifilm Europe GmbH, Duesseldorf, Germany). A 12 μm Hostaphan® film (Mitsubishi Polyester Film GmbH, Wiesbaden, Germany) was placed between the samples and the imaging plate to protect it from the labelled soil during the first imaging. This first image showed the activities of ^{137}Cs and ^{14}C , while the second imaging showed only the ^{137}Cs activity. For the second imaging, six additional plastic films (polypropylene, 40 μm thickness, density 0.95 g cm^{-3} , MDF-Verpackungen GmbH, Bergisch Gladbach, Germany) were used to shield off the ^{14}C radiation. Full shielding was checked by 1 μl drops of

activities of 125 Bq of ^{137}Cs and ^{14}C put next to the soil cuts. Exposure was three hours for both images. The imaging system FLA 5100 (Fujifilm Europe GmbH, Duesseldorf, Germany) was used to read the plates with a resolution of 100 μm . The same procedure was carried out once for each plant species for the dried and flattened leaves and stems.

Determination of exposure and shielding

The number of plastic films required for shielding off the ^{14}C β^- radiation was worked out separately. On a sheet of coated paper (DescProtect, LLG Labware GmbH, Meckenheim, Germany) 1 μl drops of dissolved $^{137}\text{CsCl}$ and ^{14}C -glucose were added at increasing activities ranging from 1 to 125 Bq. Additionally, the remaining β^- radiation of ^{137}Cs , as well as, the optimal exposure time for the imaging were determined.

Image processing

The emitted β^- radiation from the decay of ^{137}Cs and ^{14}C was stored in 16-bit digital images. The imaging plates store the signal as the quantum level (i.e. the logarithmic pixel-wise greyscale data) for each pixel. These were then converted to standardised PSL (photo-stimulated luminescence) units. This is an arbitrary unit describing the absorbed and corrected energy on the imaging plate. For the conversion, we followed the protocol given in the technical documentation of the image format (Fuji Photo Film Co. Ltd. 2003):

$$PSL = \left(\frac{P}{100}\right)^2 \times \frac{4000}{S} \times 10^{L \times \left(\frac{QL}{G} - 0.5\right)} \quad (2)$$

with:

- P the pixel size ($P = 100 \mu\text{m}$)
- QL the pixel-wise grey value (quantum level) initially stored in 16-bit images
- S the sensitivity factor ($S = 1000$)
- L the latitude ($L = 5$) and
- G related to the image format and equals to 65535 for 16-bit images.

Image processing was performed in MATLAB 2015 (The MathWorks GmbH, Ismaning, Germany). As the first step, the converted images were

normalised to get a similar background based on blank areas in the images. There were two sets of images for each plant: one capturing the decay of both ^{137}Cs and ^{14}C , and the other one showing the decay of only ^{137}Cs after shielding off the ^{14}C . Each set of images was taken separately and was, therefore, not overlapping pixel by pixel. To quantitatively separate the contributions of ^{137}Cs and ^{14}C , overlapping both sets of images enabled subtraction of the two images, i.e. the second from the first image. The two images were aligned by defining one image the reference and applying geometric transformations to the other image. For this purpose, an intensity-based image registration was used. Since the second imaging also reduced the intensity of the ^{137}Cs signal, this was corrected by calculating the attenuation from defined ^{137}Cs activities put next to the soil samples. Photos of soil cross sections were taken prior to imaging. These photos were aligned with the images obtained by imaging. Thanks to the big contrast between the roots and the soil in these photos, the roots were easily segmented from the soil through a threshold method. We focussed on the main root of each plant. A Euclidean distance map was applied to the segmented root to calculate the root radius. This distance map was used to categorise pixels around the roots according to their lateral distance from the rhizodermis, i.e. the outermost primary cell layer of the root tissue. The pixel-wise PSL values were then converted to activities (full details see next section). To calculate the radial profiles of the nuclide-specific activities as a function of the distance from the rhizodermis, mean activities were determined at given distances from the rhizodermis (Zarebanadkouki et al. 2016) - assuming radial symmetry around the roots. Summing up the increments of activities at each distance gave the total activity excreted by the root (Eq. 3).

$$A_{tot} = \sum_{i=1}^{i=n} (\pi r_i^2 - \pi r_{i-1}^2) \times A_i \quad (3)$$

with:

- A_{tot} the total activity of each nuclide excreted by the root [Bq]
- r_i the distance of a pixel i from the rhizodermis [mm] with r_0 , the root radius

A_i the mean activity of each nuclide in the distance r_i from the rhizodermis [Bq mm^{-2}]

Since different initial activities were applied to the plant species and the root diameter was different among species, we normalised the total excreted activities accordingly (Eq. 4).

$$A_{tot,norm} = \frac{A_{tot}}{A_{rcvd} \times 2\pi r_0} \quad (4)$$

with:

$A_{tot,norm}$ the normalised total activity of each nuclide [$\text{Bq Bq}^{-1} \text{mm}^{-1}$]
 A_{tot} the total activity of each nuclide excreted by the root [Bq]
 A_{rcvd} the total activity of a nuclide recovered in a pot and shoot
 r_0 the root radius

Quantification of the images

The pixel-wise PSL values were converted to ^{137}Cs and ^{14}C activities by a regression describing the relation between the PSL values and the activities of ^{137}Cs and ^{14}C standards. The regression function was obtained by imaging known activities of ^{137}Cs and ^{14}C . For this, 0.5 g of the soil from the plant experiment were adjusted to 25% soil moisture (gravimetric) by dropwise addition of 150 μl of dissolved ^{14}C -glucose and ^{137}Cs activities ranging from 20 to 325 $\text{Bq } \mu\text{l}^{-1}$. The soil was mixed to achieve a uniform mixture and transferred to a 96-well microtiter plate (U-shaped wells with a diameter of 6.94 mm and a depth of 11.65 mm; Brandplates®, Brand GmbH + Co KG Wertheim, Germany). A smooth soil surface was prepared on the level of the rim of each cup. Aliquots of ^{14}C -glucose were dissolved in Rotiszint® eco plus scintillation cocktail (Carl Roth GmbH + Co. KG, Karlsruhe, Germany) and activities were determined by the liquid scintillation counter Tricarb™ B3180 TR/SL (PerkinElmer Inc., Waltham, MA, U.S.A.). Activities of ^{137}Cs were measured on the HiDex Automatic Gamma counter. The images were normalised to the background and emitted energies were converted to PSL values. The ^{137}Cs and ^{14}C activities and their

PSL values were normalised to the applied areas and a linear function was fitted to the PSL values.

Spatial overlap of ^{137}Cs and ^{14}C hot spots

The quantified and ready images of ^{137}Cs and ^{14}C were taken and the spatial overlap (r) of the main activities was estimated by the spatial overlap coefficient (Eq. 5) (Bolte and Cordelières 2006; Manders et al. 1993). This was performed by means of the JACoP plugin (Cordelières and Bolte 2009) in Fiji (Schindelin et al. 2012; Schindelin et al. 2015) using manually set thresholds.

$$r = \frac{\sum_i A_i \times B_i}{\sqrt{\sum_i (A_i)^2 \times \sum_i (B_i)^2}} \quad (5)$$

with:

A the intensities of a pixel of channel A,
 B the intensities of the corresponding pixel of channel B

Determination of ^{137}Cs and ^{14}C bulk activities

At the end of the experiment, all soil was collected, plants were cut above ground and the dry weight of the soil and shoots were determined after drying at 75 °C for 120 h. Visible, larger roots were pre-ground separately in a ball mill (PM 100; Retsch, Haan, Germany) for at least 15 min prior to adding the soil and milling for another 15 min. Five replicates of ~1 g of soil and roots were taken and ^{137}Cs γ activity was measured. The same samples were incinerated at 500 °C and the resulting $^{14}\text{CO}_2$ was trapped in Oxysolve C-400 scintillation cocktail (Zinsser Analytic GmbH, Frankfurt, Germany) prior to the scintillation measurement.

The belowground tracer allocation was expressed as the belowground activity relative to the total recovered activity (shown for ^{137}Cs in Eq. 6a). The aboveground allocation was

calculated as the aboveground activity relative to the total activity recovered (shown for ^{14}C in Eq. 6b).

$$^{137}\text{C}_{\text{belowground}} = \frac{\sum_{i=1}^n \frac{^{137}\text{C}_{\text{belowground},i}}{(^{137}\text{C}_{\text{aboveground},i} + ^{137}\text{C}_{\text{belowground},i})}}{n} \times 100\% \quad (6a)$$

with:

$^{137}\text{C}_{\text{belowground}}$	the mean belowground ^{137}C allocation of a plant species [%]
$^{137}\text{C}_{\text{belowground},i}$	the recovered belowground ^{137}C activity of a replicate i , i.e. soil and roots [kBq]
$^{137}\text{C}_{\text{aboveground},i}$	the ^{137}C activity recovered in the shoot of a replicate i [kBq]
n	the number of replicates

$$^{14}\text{C}_{\text{aboveground}} = \frac{\sum_{i=1}^n \frac{^{14}\text{C}_{\text{aboveground},i}}{(^{14}\text{C}_{\text{aboveground},i} + ^{14}\text{C}_{\text{belowground},i})}}{n} \times 100\% \quad (6b)$$

with:

$^{14}\text{C}_{\text{aboveground}}$	the mean aboveground ^{14}C allocation of a plant species [%]
$^{14}\text{C}_{\text{belowground},i}$	the belowground ^{14}C activity recovered in a replicate i , i.e. roots and soil [kBq]
$^{14}\text{C}_{\text{aboveground},i}$	the ^{14}C activity recovered in the shoot of a replicate i [kBq]
n	the number of replicates

Results

Labelling with ^{137}C and ^{14}C

^{137}C transported within the leaves of both plant species was detectable 6 h after labelling had started using a Geiger-Müller counter with a small probe. Presence of ^{137}C in the roots, i.e. at the bottom of pots, was detectable two days after labelling. Imaging confirmed that

strongly increased ^{137}C activities were allocated to the more distal parts within four days in the case of both plant species, e.g. in young leaves and leaf bases of chicory (Online Resources 2 and 3). ^{137}C uptake was $98.0 \pm 0.8\%$ for chicory and $99.8 \pm 0.1\%$ for alfalfa (Table 1). Root allocation of ^{137}C did not strongly depend on the plant species: chicory allocated $9.4 \pm 1.5\%$ and alfalfa allocated $7.1 \pm 1.6\%$ of the tracer below ground (Table 1). Even after four days, more than 90% of the ^{137}C was still in the shoot, which is also discernible in the imaging of the shoot (Online Resources 2 and 3).

Imaging revealed that the ^{14}C β^- radiation was completely shielded to the background level by six layers of 40 μm polypropylene film and one layer of 12 μm Hostaphan® film (Online resource 7). Shielding attenuated the ^{137}C radiation by $35.8 \pm 1.5\%$.

The ^{137}C and ^{14}C labelling technique and its feasibility will be first illustrated exemplarily for two replicates per species. Detailed images of all pots are given as Online Resources 4 and 5. The example images of both species are shown in Fig. 2, in which the intensities correspond to the quantum level, i.e. the logarithmic pixel-wise greyscale data. Both plants, roots and their rhizosphere showed strongly increased activities of ^{137}C and ^{14}C and therefore, their spatial distribution can be easily distinguished. Pixel-wise subtraction of ^{137}C images from the images of total ^{137}C and ^{14}C activity gave the ^{14}C contribution (Fig. 3). Here, subtracting the ^{137}C image from the total image worked remarkably well and resulted in two separate datasets of ^{137}C and ^{14}C , which was the main aim of this experiment. Both radionuclide distributions gave good representations of the roots (Fig. 2, top and below, Online Resources 4 and 5), including the prominent main roots and laterals (chicory), as well as secondary roots (alfalfa). Congruence of the main root locations by both radionuclide distributions was very high as determined by the overlap coefficient with $96.0 \pm 1.1\%$ for chicory and $95.3\% \pm 0.9\%$ for alfalfa.

Quantification of the intensities

The two separated radionuclide visualisations were quantified by a regression function, which described the linear relation between PSL value and the activities of each radionuclide ($R^2 > 0.98$, Fig. 4). For further quantifications, we focussed on the main root of each plant. Radial distributions of ^{137}C and ^{14}C activities as

Table 1 ^{137}Cs and ^{14}C budget. Shown are means of five replicates \pm standard errors of the mean

	^{137}Cs uptake	^{137}Cs aboveground	^{137}Cs belowground	^{14}C aboveground	^{14}C belowground
	[%]	[%] of recovery	[%] of recovery	[%] of recovery	[%] of recovery
Chicory	98.0 \pm 0.8	90.6 \pm 1.5	9.4 \pm 1.5	37.4 \pm 4.5	62.6 \pm 4.5
Alfalfa	99.8 \pm 0.1	92.9 \pm 1.6	7.1 \pm 1.6	79.4 \pm 6.0	20.6 \pm 6.0

a function of distance from the rhizodermis are given in Fig. 5. For both plants, the activities were higher near the rhizodermis and decreased towards the bulk soil. In general, the ^{137}Cs activity at the rhizodermis was about 4–5 times higher than the activity of ^{14}C . The radial extension of ^{137}Cs was also larger in both plants than the ^{14}C (e.g. alfalfa, ca. 0.25 cm vs. 0.15 cm). The rhizosphere extensions of ^{137}Cs and ^{14}C were about 40% smaller in the case of alfalfa compared to chicory. The two plant species initially received different total activities and their roots had different diameters. Therefore, Fig. 6 shows activities normalised to the total recovered activities and root perimeter: chicory excreted \sim 23 times more ^{14}C and 15 times more ^{137}Cs than alfalfa. Both species gave more ^{137}Cs than ^{14}C into the rhizosphere at 5 cm depth. So, the excretion of nuclides depended on the plant species and the type of nuclide.

Discussion

The double labelling approach

We presented a proof-of-concept, which should enable the visualisation and quantification of the reuse of biopores (Fig. 1). Our approach simulates the path of the Chernobyl ^{137}Cs fallout from the leaves into the roots by labelling crops through the leaves with $^{137}\text{CsCl}$ to create ^{137}Cs -labelled root biopores. The roots of the subsequently grown crop could then be differentiated by $^{14}\text{CO}_2$ labelling to create ^{14}C -labelled roots. The feasibility of our concept was shown in an experiment, in which the same plants were labelled by both tracers. This simulates the situation of a re-used root channel, i.e. both radionuclides spatially overlapping in the same root channel.

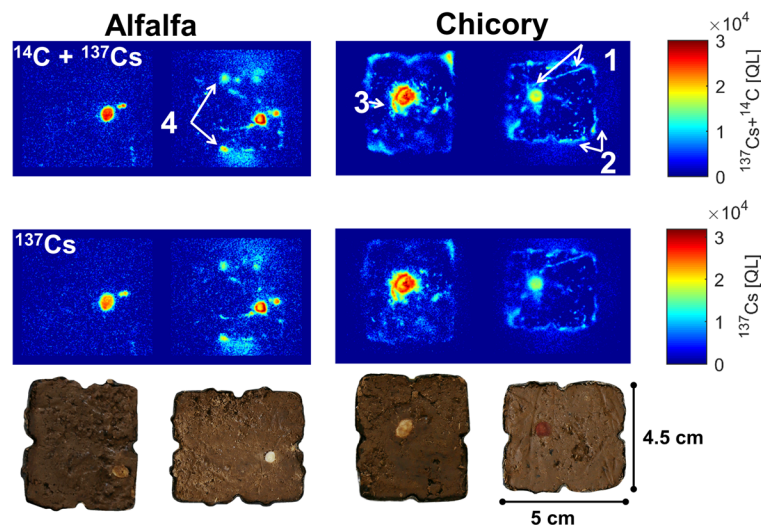
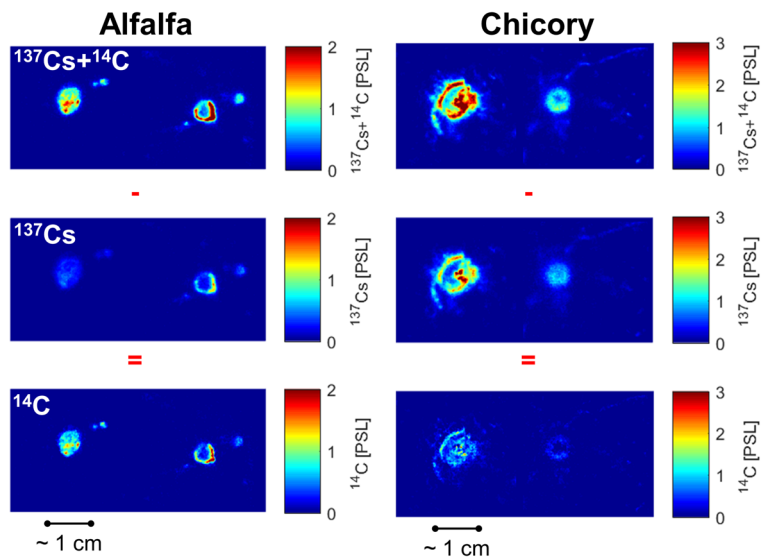


Fig. 2 Imaging of ^{137}Cs and ^{14}C (top) and ^{137}Cs only (middle) activities in the soil at a depth of 5 cm for alfalfa (left) and chicory (right). Below the imagings are rotated photos of the respective soil cuts. The images presented quantum level data (QL, i.e. the pixel-wise grey values stored in 16-bit images) which was initially captured during imaging. The red colour corresponds to higher activities. Note, that here two plants are given as examples and all

plants are given as supplementary information (Online Resources 4 and 5). Numeric identifiers and arrows relate to 1) lateral root emerging from the single tap root of chicory, 2) a large number of fine roots growing in the gap between the soil and the container, 3) sloughed off rhizodermis, and 4) smaller secondary roots as opposed to chicory's taproot

Fig. 3 Procedure of image processing after conversion to PSL units and successful subtraction of ^{137}Cs activity (middle) of total activity (top) to yield the ^{14}C activity (bottom), shown for two examples of the largest, i.e. main roots, to which a colour map was applied



Applying ^{137}Cs and ^{14}C to plants was easy, fast and straightforward. Labelling plants with $^{14}\text{CO}_2$ and ^{14}C -photosynthate release into the soil is well established (Pausch and Kuzyakov 2011). There were earlier hints that the labelling with ^{137}Cs might be feasible: ^{137}Cs from seedlings incubated in $^{137}\text{CsCl}$ solution was released from their roots into the ^{137}Cs -free soil (Bystrzejewska-Piotrowska and Urban 2004). Of the total ^{137}Cs activity, 7.1–9.4% was allocated below ground within four days (Table 1). At least four reasons explain why the ^{137}Cs labelling worked remarkably well: I) the absence of uptake-regulating barriers in cut leaves and stems as compared to roots (e.g. Casparian strip in the root endodermis), II) the comparatively high mobility of caesium in plants (Online Resources 1 and 2; Bystrzejewska-Piotrowska and Urban 2004), III) its similarity to K and, therefore, possibly selective uptake,

and IV) the translocation of it to the roots through the phloem (Buisse et al. 1995; Zhu and Smolders 2000). It may be speculated that the ^{137}Cs uptake follows the uptake mechanisms of other cations, i.e. uptake through the cut surface or stomata, or cuticular penetration (Fernández and Eichert 2009; Stock and Holloway 1993). The contributions of the three mechanisms for the two species cannot be estimated from our data. However, we found evidence of selective uptake of ^{137}Cs by chicory. Almost all ^{137}Cs activity was taken up from the tracer solution (Table 1). Yet, there was still solution present at the end of the experiment in the chicory vials, which contained ^{137}Cs activities lower than the ^{137}Cs activity expected in the remaining volume. Hence, we assume selective uptake of Cs compared to water, most probably since Cs is a K analogue.

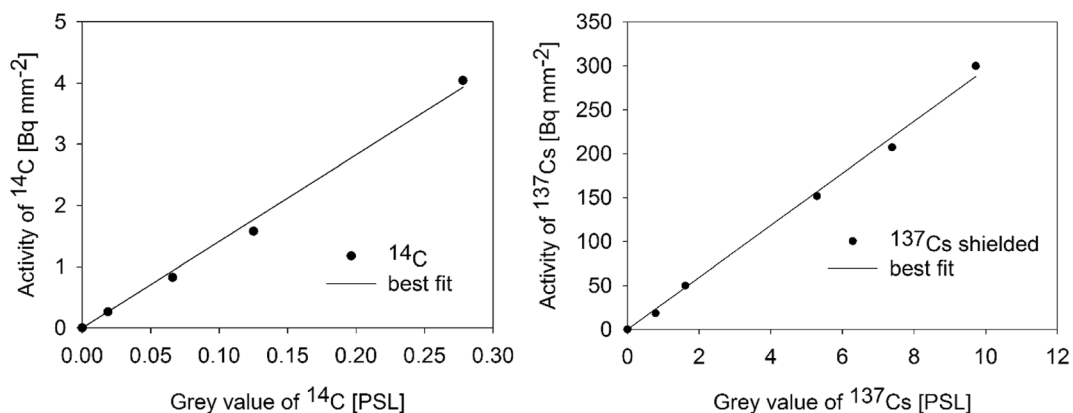


Fig. 4 Standardisation of ^{137}Cs and ^{14}C activities and their PSL (photo-stimulated luminescence) values by linear regression

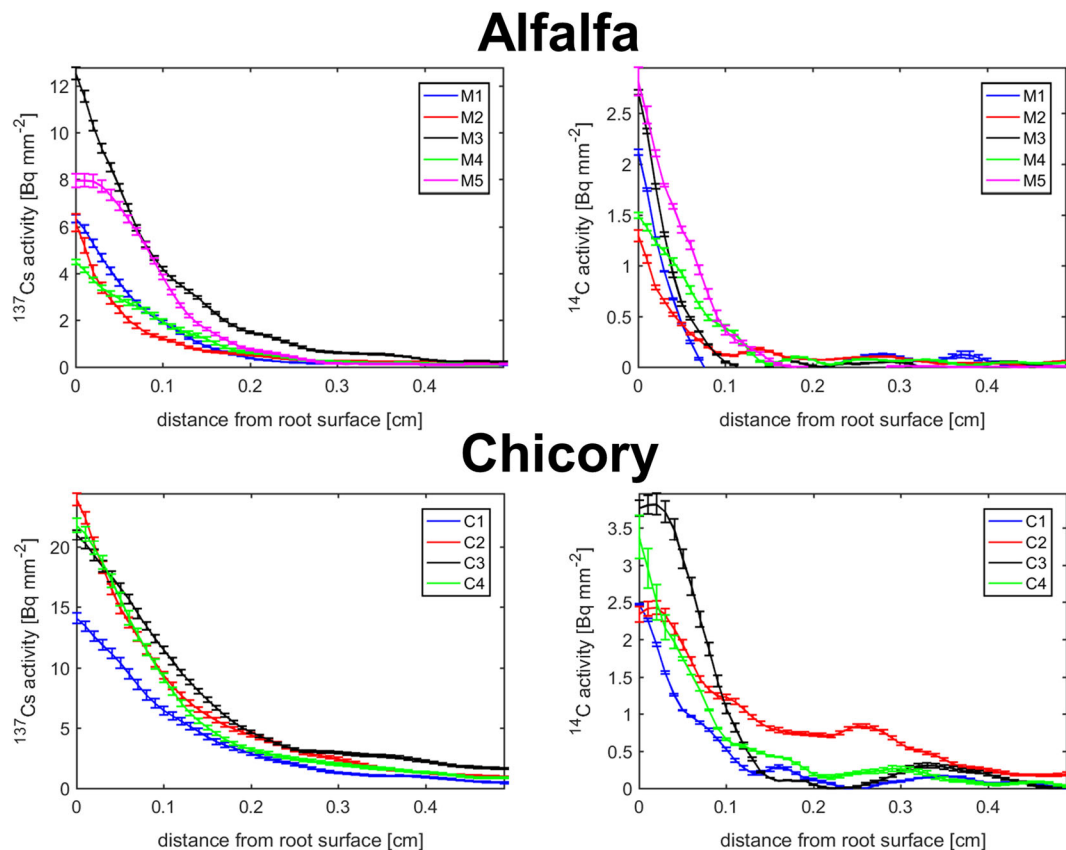


Fig. 5 Radial profiles of ^{137}Cs (left) and ^{14}C (right) activities as a function of the distance from the rhizodermis for five alfalfa replicates (top) and four chicory replicates (bottom). Data averaged in radial

direction around (360°) the largest root of each plant. Error bars show the variance of the activities (as standard errors) in the respective distance from the rhizodermis

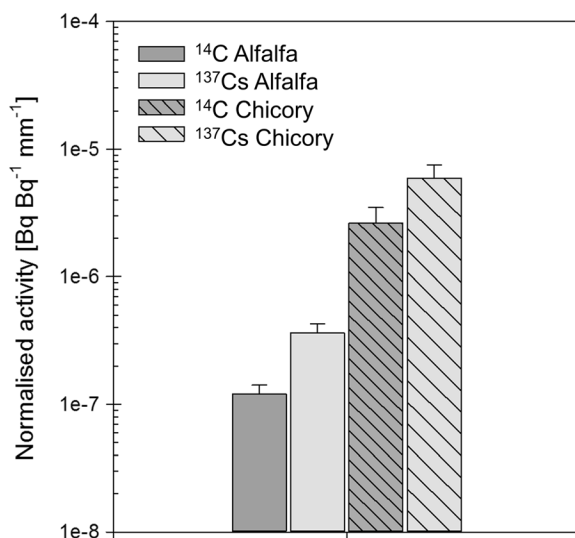


Fig. 6 Total ^{137}Cs and ^{14}C activities in the rhizosphere of alfalfa and chicory obtained from Eq. 4, i.e. normalised by the total activities taken up by each plant and the root perimeter. The data are averaged among replicates and error bars show standard errors

The belowground allocation induced very strong signals in the soil - far above the detection limit and the background luminescence of the imaging plate. Herein, we focussed on the main roots, which turn into biopores desirable in organic agriculture (Kautz et al. 2013), but finer roots were also labelled. The main challenge was to prove that both nuclides were individually detectable. This required separation of ^{137}Cs and ^{14}C β^- radiation signals, which was achieved by shielding during the two-step imaging procedure (Fig. 3, Online Resource 7). It was shown that the root release of radionuclides could be used to visualise roots, their locations and features such as laterals or secondary roots - irrespective of the species (Fig. 2). After labelling, the ^{137}Cs distribution in the rhizosphere represents the Cs^+ and K^+ excretion from the roots from the start of the labelling to imaging. Also, it gives the size distribution of the roots and later biopores in a soil cut. ^{14}C -photosynthates in the rhizosphere are representative of the root exudation of low molecular organic substances. Like ^{137}Cs ,

the ^{14}C activity distribution gives the size, extension and locations of the roots (Fig. 3). Consequently, the size distribution and count data of roots and biopores of both fibrous and tap-rooted plants could be determined and compared. The descriptive statistics are needed as a foundation for future research.

Our experiment has shown, that both radionuclides were allocated below ground, gave satisfying representations of the roots and the strong signals were successfully separated from each other through shielding during imaging (Fig. 3). The low mobility of ^{137}Cs in soil and its long half-life of about 30 years are well-established properties and should lead to stable labelling of biopores (Cremers et al. 1988; Walling and Quine 1995). Also, the rhizodeposition of ^{14}C -photosynthates is frequently and successfully applied. With these prerequisites met, biopore reuse quantification comes within reach.

Implications for biopore reuse

The reuse of pre-crop biopores in crop rotations by subsequently grown main crops is obvious (Elkins 1985; Han et al. 2016), but has not been quantified yet due to a lack of methods. Although not specifically tested herein, our approach should be feasible for biopore studies. Even under the assumption, that only low ^{137}Cs activities were excreted by the roots within four days, the signal was already strong enough for imaging (Fig. 2). The exact ^{137}Cs activities excreted are only of secondary importance in this regard. As long as ^{137}Cs is translocated into the roots prior to root death, it will be released into the developing root channel upon cell death and during root decomposition. Hypothetically and according to our concept, after the main crop phase in a crop rotation, unused biopores would feature only ^{137}Cs , while reused biopores would show a spatial overlap of ^{137}Cs and ^{14}C activities. Finally, roots growing in bulk soil would be only labelled with ^{14}C and not with ^{137}Cs . In principle, earthworm biopores could also be labelled by feeding earthworms ^{137}Cs - or ^{14}C -labelled litter, which would enable more earthworm-related research opportunities. ^{14}C and bomb-fallout ^{137}Cs were already shown to be possible tools to determine the age of individual burrows, bioturbation and organic matter turnover (Cheshire and Griffiths 1989; Hasegawa et al. 2013; VandenBygaert et al. 1998).

We presented one approach to quantify the ^{137}Cs and ^{14}C signals to later quantify biopore reuse from the

imaging: the overlap coefficient (Bolte and Cordelières 2006; Manders et al. 1993). Since both labellings were performed on the same plants without waiting for root decomposition after the pre-crop phase, all ^{137}Cs -labelled roots were also labelled with ^{14}C (Fig. 3). This is discernible from the high overlap coefficient of >0.95 .

Further applications

This dual labelling approach could be particularly useful to localise and visualise further processes on different scales: on the smaller rhizosphere scale, estimating the rhizosphere extension of organic and inorganic substances, and on a larger scale, the root system architecture.

Extension of photosynthates and solutes' diffusion in the rhizosphere: the rhizosphere boundary

As the highest ^{137}Cs and ^{14}C activities were located around the main roots, i.e. the tap roots and largest fibrous roots, these were considered the main regions of interest (Fig. 2). Radial distributions of ^{137}Cs and ^{14}C starting from the rhizodermis into the bulk soil are shown in Fig. 5. The distance of the rhizodermis to the point where the activity was for the first time down to 5% of the activity of the root centre was defined as the rhizosphere extension. This definition is rather arbitrary since it only serves the purpose of showing the feasibility of the approach also in the narrow rhizosphere: heterogeneous rhizodeposition patterns in varying soil depths can be determined easily.

The radionuclide localisation and activity distribution explain I) the pattern of the gradients and II) the amount of tracer excreted by the root. Radionuclide-specific rhizosphere extensions were expected according to the size and charge of the excreted compounds (Fig. 5). $^{137}\text{Cs}^+$ strongly binds to iron oxides and clays (Giannakopoulou et al. 2007; Riise et al. 1990) and is not taken up by microorganisms in large amounts like C, e.g. as an energy source. This results in a ^{137}Cs rhizosphere extension which is monotonically decreasing. The ^{137}Cs distribution represents the microbially non-decomposable release of K. On the contrary, ^{14}C -labelled photosynthates are taken up very fast and efficiently by microorganisms (Fischer et al. 2010), respired, used for biofilm formation or stabilised as necromass (Miltner et al. 2012). The locations of such

processes are clearly visible in Fig. 5 as the distribution of ^{14}C increases and decreases within the rhizosphere. The radial distribution of ^{14}C was also similar to the distribution of enzyme activities in the rhizosphere (Razavi et al. 2016). Apart from these lateral patterns, exudation along the roots could be studied by cutting the soil cores either horizontally at different depths, by cutting it vertically or by using rhizotrons (Razavi et al. 2016).

Separating and quantifying radionuclides in the rhizosphere on a resolution of 100 μm was accomplished (Fig. 3). Enhancing the resolution to 25 μm is possible and will capture finer details and more exact rhizosphere extensions. Utilising the ^{14}C activity as a proxy for organic compounds in the rhizosphere will help elucidate C dynamics in root-induced hot spots (Pausch and Kuzyakov 2011). ^{137}Cs as an analogue for the nutrient potassium could be a new tool not just for biopore reuse but also a proxy for solute excretion from roots. To our knowledge, there is no tool available yet to quantitatively visualise the rhizosphere dynamics of both root exudates and solutes in situ. We, therefore, propose this radionuclide imaging/shielding approach, which should in principle also work with ^{40}K , ^{90}Sr (as an analogue for Ca), ^{36}Cl , ^{35}S or ^{33}P . Changing the radionuclides would also enable to study other processes or elements, e.g. behaviour of anions in the rhizosphere.

Root system architecture

Albeit the biopore reuse was our prime interest, the approach may also be useful to study the root system architecture. Herein, the soil core was cut once in 5 cm depth. By increasing the number of cuts, one may be able to get a 3D approximation of the root system. Additionally, extra vertical cuts could be helpful for modelling. Repeated pulses of ^{14}C and ^{137}Cs ensure that the roots are homogeneously labelled. Compared to computer tomography, this approach may be less accurate and needs destructive sampling, but it is certainly more affordable.

Methodological recommendations

It is recommended to label the first crop with ^{137}Cs and the subsequent crop with ^{14}C due to the rapid microbial C turnover in the rhizosphere and fast losses as $^{14}\text{CO}_2$ compared to ^{137}Cs . If biopore reuse of further crops appears interesting, a third crop could be labelled with radionuclides having maximum β^- decay energies

not too close to 156 or 514 keV, such as ^{40}K (1.31 MeV) or ^{36}Cl (0.71 MeV). In case extremely high activities are used, an overflow effect may occur, i.e. very high activities paired with long exposure times may cause unproportional luminescence on the imaging plates. We have not found this to impact the image quality in our setup. If this effect occurs, two measures could help to maintain a high localising resolution: I) keeping the distance between the soil and imaging plate as small as possible and II) 3D collimators or anti-scatter grids cutting off scattered radiation.

High CsCl concentrations in plants may inhibit photosynthesis and may cause contractile roots in young plants (Bystrzejewska-Piotrowska et al. 2004). Even though the actual ^{137}Cs tracer concentrations are orders of magnitude too low to cause such effects, we recommend high activities of the ^{137}Cs tracer and lowest concentrations of a $^{133}\text{CsCl}$ medium. Mature plants are expected to be less affected by salinity as compared to young plants (Hasegawa et al. 2015). Leaves of our 200 day-old plants did not show any colour changes at CsCl concentration of 0.5 mM. Chicory leaves were left in the ^{137}Cs solution for up to 48 h without visible damage. In a different pre-test (not shown), damages were observed after >48 h, but this may vary for different species or growth stages. We, therefore, recommend pre-tests with the desired plant species and unlabelled solutions. The unlabelled CsCl medium is also required to handle the ^{137}Cs , as its actual concentration would be too small to handle: the slightest contamination with clay or iron oxides in a tracer solution without ^{133}Cs would bind a large part of the ^{137}Cs .

For the leaf-feeding, cutting the leaves under water and adding a surfactant such as Silwet® Gold (Spiess-Urania, Hamburg, Germany) to the CsCl solution may further reduce the risk of unsuccessful labellings caused by embolies. If performed in the field, the leaf feeding procedure may be carried out like in the laboratory, i.e. cutting the leaves and immersing them in a solution of tracer and surfactant. Repeated ^{137}Cs pulse labelling at different growth stages is expected to label the root pores more homogeneously in deeper soil layers.

$^{14}\text{CO}_2$ pulse labelling is regularly performed and specific issues were reviewed extensively elsewhere (Kuzyakov and Domanski 2000; Meharg 1994). Due to rapid C turnover in soil and rhizosphere, the imaging procedure should be carried out as soon as possible after the second, i.e. ^{14}C labelling, to receive the strongest ^{14}C signals. In the field, the $^{14}\text{CO}_2$ labelling can be

performed in a portable plastic chamber similar to our laboratory setup (Hafner and Kuzyakov 2016). In the field and unlike in this experiment, roots will not be as concentrated as in our pots, but rather be more dispersed. One countermeasure could be to use larger imaging plates (i.e. maximum 35×43 cm with our manufacturer). Also, the signals may be weaker because of a higher root mass and, therefore, possibly lower ^{137}Cs activity per rhizodermis. To maintain a high image quality, two measures are recommended: I) repeated pulse labelling of both nuclides (cf. above) and II) longer exposure.

For easier cutting of the soil cores, we adjusted the water content to 45–50% of the maximum water holding capacity. Freezing the soil cores could also be a suitable approach to avoid the redistribution of soil particles during the cutting (Kuzyakov et al. 2003). However, care should be taken not to cause excessive stress on the surrounding soil. Regarding occupational health and safety, during the cutting and handling of the soil and solutions in the lab, we strongly recommend to always follow common radiation protection rules to keep radiation exposure as low as reasonably achievable. Incorporation of ^{137}Cs -contaminated soil dust could be minimised by wearing face masks and performing dust-producing tasks in a fume hood.

Some issues are conceivable and may need consideration when scaling this proof-of-concept up to a crop rotation – since this was not yet tested. The largest difference between this experiment and a crop rotation would be the duration of root decomposition and with this comes a range of issues regarding the feasibility of the approach. First, ^{137}Cs release upon root cell death needs to be shown. In soils with a high biotic activity, the signals might be disturbed in the long run: even though ^{137}Cs should not diffuse away from mineral surfaces, soil particles may be pushed away by earthworms or roots. For instance, secondary thickening or growth of thicker main crop roots may be expected to weakly impact the positions of ^{137}Cs signals by slightly pushing soil particles away from their former position. Even if the main crops pushed ^{137}Cs -labelled soil away, e.g. in the case of a fibrous pre-crop and a tap-rooted main crop, spatial overlap of ^{137}Cs and ^{14}C would still be expected. In the opposite case, i.e. the main crop features small roots compared to the biopore diameter, the main crop ^{14}C signal may be small. In

this case, multiple pulse or continuous labelling is recommended. It, however, remains to be determined if these effects are relevant for the time frame of root decomposition in a crop rotation.

Conclusions

A new dual labelling approach with foliar application of ^{137}Cs and ^{14}C and selective shielding during the imaging of soil cuts was successfully tested: more than 99% of the ^{137}Cs tracer was taken up irrespective of the plant species and of this 7.1–9.4% were allocated below ground within four days. β^- radiation around the roots proved that both ^{137}Cs and ^{14}C were released into the rhizosphere, effectively creating roots labelled with both ^{137}Cs and ^{14}C . Shielding successfully separated the two signals. Albeit not specifically tested herein, if the two tracers are applied to separate, subsequent crops in a crop rotation, the ultimate goal of biopore reuse quantification appears feasible: the long half-life of ^{137}Cs , its relatively high energy β^- radiation and very low mobility in soil should enable stable and long-term labelling of rhizosphere soil and, after decomposition, root biopores. Labelling main crops with ^{14}C would enable quantification of the reuse of root biopores and would help estimate their importance over longer periods and on larger scales – possibly under field conditions. We conclude that ^{137}Cs can be a useful proxy of biopore reuse and possibly for the extent of solute dynamics in the rhizosphere and root system architecture studies.

Acknowledgements This study was supported by the German Research Foundation (KU 1184/29-1). We would like to thank Gabriele Lehmann and Rainer Schulz of the Laboratory for Radioisotopes (LARI) of the University of Goettingen for their advice, support and measurements.

Compliance with ethical standards

Conflicts of interest The authors declare no conflicts of interest.

References

- Amato E, Lizio D (2009) Plastic materials as a radiation shield for β^- sources. A comparative study through Monte Carlo calculation. *J Radiol Prot* 29:239–250

- Athmann M, Kautz T, Pude R, Köpke U (2013) Root growth in biopores—evaluation with in situ endoscopy. *Plant Soil* 371: 179–190
- Banfield CC, Dippold MA, Pausch J, Hoang DTT, Kuzyakov Y (2017) Biopore history determines the microbial community composition in subsoil hotspots. *Biol Fertil Soils* 1–16. doi:10.1007/s00374-017-1201-5
- Bolte S, Cordelières FP (2006) A guided tour into subcellular colocalization analysis in light microscopy. *J Microsc* 224: 213–232
- Buysse J, den Brande V, Karen MR (1995) The distribution of Radiocesium and potassium in spinach plants grown at different shoot temperatures. *J Plant Physiol* 146:263–267
- Bystrzejewska-Piotrowska G, Urban PL (2004) Accumulation and translocation of cesium-137 in onion plants (*Allium cepa*). *Environ Exp Bot* 51:3–7
- Bystrzejewska-Piotrowska G, Jeruzalski M, Urban PL (2004) Uptake and distribution of caesium and its influence on the physiological processes in croton plants (*Codiaeum variegatum*). *Nukleonika* 49:35–38
- Carminati A (2013) Rhizosphere wettability decreases with root age: a problem or a strategy to increase water uptake of young roots? *Front Plant Sci* 4:298
- Cheshire MV, Griffiths BS (1989) The influence of earthworms and cranefly larvae on the decomposition of uniformly ¹⁴C labelled plant material in soil. *J Soil Sci* 40:117–124
- Cordelières FP, Bolte S (2009) JACoP v2.0: improving the user experience with co-localization studies. Proceedings of the 2nd ImageJ user and developer conference 2008:174–181
- Cremers A, Elsen A, Preter PD, Maes A (1988) Quantitative analysis of radiocaesium retention in soils. *Nature* 335:247–249
- Dippold MA, Kuzyakov Y (2016) Direct incorporation of fatty acids into microbial phospholipids in soils: position-specific labeling tells the story. *Geochim Cosmochim Acta* 174:211–221
- Ehlers W, Köpke U, Hesse F, Böhm W (1983) Penetration resistance and root growth of oats in tilled and untilled loess soil. *Soil Tillage Res* 3:261–275
- Elkins CB (1985) Plant roots as tillage tools. *J Terramech* 22:177–178
- Fernández V, Eichert T (2009) Uptake of hydrophilic solutes through plant leaves. Current state of knowledge and perspectives of foliar fertilization. *Crit Rev Plant Sci* 28:36–68
- Fischer H, Ingwersen J, Kuzyakov Y (2010) Microbial uptake of low-molecular-weight organic substances out-competes sorption in soil. *Eur J Soil Sci* 61:504–513
- Giannakopoulou F, Haidouti C, Chronopoulou A, Gasparatos D (2007) Sorption behavior of cesium on various soils under different pH levels. *J Hazard Mater* 149:553–556
- Gunina A, Dippold MA, Glaser B, Kuzyakov Y (2014) Fate of low molecular weight organic substances in an arable soil: from microbial uptake to utilisation and stabilisation. *Soil Biol Biochem* 77:304–313
- Hafner S, Kuzyakov Y (2016) Carbon input and partitioning in subsoil by chicory and alfalfa. *Plant Soil* 406:29–42
- Hagedorn F, Bundt M (2002) The age of preferential flow paths. *Geoderma* 108:119–132
- Han E, Kautz T, Perkons U, Uteau D, Peth S, Huang N, Horn R, Köpke U (2015) Root growth dynamics inside and outside of soil biopores as affected by crop sequence determined with the profile wall method. *Biol Fertil Soils* 51:847–856
- Han E, Kautz T, Köpke U (2016) Precrop root system determines root diameter of subsequent crop. *Biol Fertil Soils* 52:113–118
- Hasegawa M, Ito MT, Kaneko S, Kiyono Y, Ikeda S, Makino S (2013) Radiocesium concentrations in epigeic earthworms at various distances from the Fukushima nuclear power plant 6 months after the 2011 accident. *J Environ Radioact* 126:8–13
- Hasegawa H, Tsukada H, Kawabata H, Takaku Y, Hisamatsu S (2015) Foliar uptake and translocation of stable Cs and I in radish plants. *J Radioanal Nucl Chem* 303:1409–1412
- Hiltner L (1904) Über neuere Erfahrungen und Probleme auf dem Gebiete der Bodenbakteriologie unter besonderer Berücksichtigung der Gründüngung und Brache. *Arbeiten der Deutschen Landwirtschaftlichen Gesellschaft* 98:59–78
- Hirth JR, McKenzie BM, Tisdall JM (2005) Ability of seedling roots of *Lolium perenne* L. to penetrate soil from artificial biopores is modified by soil bulk density, biopore angle and biopore relief. *Plant Soil* 272:327–336
- Hoang DTT, Pausch J, Razavi BS, Kuzyakova I, Banfield CC, Kuzyakov Y (2016) Hotspots of microbial activity induced by earthworm burrows, old root channels, and their combination in subsoil. *Biol Fertil Soils* 52:1105–1119
- Jones DL, Nguyen C, Finlay RD (2009) Carbon flow in the rhizosphere: carbon trading at the soil–root interface. *Plant Soil* 321:5–33
- Kautz T, Amelung W, Ewert F, Gaiser T, Horn R, Jahn R, Javaux M, Kemna A, Kuzyakov Y, Munch J-C, Pätzold S, Peth S, Scherer HW, Schloter M, Schneider H, Vanderborght J, Vetterlein D, Walter A, Wiesenberg GL, Köpke U (2013) Nutrient acquisition from arable subsoils in temperate climates: a review. *Soil Biol Biochem* 57:1003–1022
- Kuzyakov Y, Blagodatskaya E (2015) Microbial hotspots and hot moments in soil: concept & review. *Soil Biol Biochem* 83: 184–199
- Kuzyakov Y, Domanski G (2000) Carbon input by plants into the soil. Review. *J Plant Nutr Soil Sci* 163:421–431
- Kuzyakov Y, Raskatov A, Kaupenjohann M (2003) Turnover and distribution of root exudates of *Zea mays*. *Plant Soil* 254: 317–327
- Manders EM, Verbeek FJ, Aten JA (1993) Measurement of colocalization of objects in dual-colour confocal images. *J Microsc* 169:375–382
- Meharg AA (1994) A critical review of labelling techniques used to quantify rhizosphere carbon-flow. *Plant Soil* 166:55–62
- Miltner A, Bombach P, Schmidt-Brücken B, Kästner M (2012) SOM genesis: microbial biomass as a significant source. *Biogeochemistry* 111:41–55
- Nucleonica GmbH (2014) Nucleonica Nuclear Science Portal (www.nucleonica.com). Karlsruhe, Germany. https://www.nucleonica.com/wiki/index.php?title=How_do_I_reference_Nucleonica_in_Scientific_Publications
- Paterson E (2003) Importance of rhizodeposition in the coupling of plant and microbial productivity. *Eur J Soil Sci* 54:741–750
- Pausch J, Kuzyakov Y (2011) Photoassimilate allocation and dynamics of hotspots in roots visualized by ¹⁴C phosphor imaging. *J Plant Nutr Soil Sci* 174:12–19
- Razavi BS, Zarebanadkouki M, Blagodatskaya E, Kuzyakov Y (2016) Rhizosphere shape of lentil and maize. Spatial distribution of enzyme activities. *Soil Biol Biochem* 96:229–237
- Riise G, Bjørnstad HE, Lien HN, Oughton DH, Salbu B (1990) A study on radionuclide association with soil components using

- a sequential extraction procedure. *J Radioanal Nucl Chem Artic* 142:531–538
- Schindelin J, Arganda-Carreras I, Frise E, Kaynig V, Longair M, Pietzsch T, Preibisch S, Rueden C, Saalfeld S, Schmid B, Tinevez J-Y, White DJ, Hartenstein V, Eliceiri K, Tomancak P, Cardona A (2012) Fiji: an open-source platform for biological-image analysis. *Nat Methods* 9:676–682
- Schindelin J, Rueden CT, Hiner MC, Eliceiri KW (2015) The ImageJ ecosystem: an open platform for biomedical image analysis. *Mol Reprod Dev* 82:518–529
- Schuller P, Voigt G, Handl J, Ellies A, Oliva L (2002) Global weapons' fallout ¹³⁷Cs in soils and transfer to vegetation in south-central Chile. *J Environ Radioact* 62:181–193
- Stock D, Holloway PJ (1993) Possible mechanisms for surfactant-induced foliar uptake of agrochemicals. *Pestic Sci* 38:165–177
- UNSCEAR (2011) Sources and effects of ionizing radiation. UNSCEAR 2008 report to the general assembly, with scientific annexes: volume II: effects, annex. D. United Nations, New York
- VandenBygaert AJ, Protz R, Tomlin AD, Miller JJ (1998) ¹³⁷Cs as an indicator of earthworm activity in soils. *Appl Soil Ecol* 9:167–173
- Walling DE, He Q (1999) Improved models for estimating soil erosion rates from cesium-137 measurements. *J Environ Qual* 28:611–622
- Walling DE, Quine T (1995) Use of fallout radionuclide measurements in soil erosion investigations. In: IAEA (ed), nuclear techniques in soil plant studies for sustainable agriculture and environmental preservation. Proceedings of an international symposium on nuclear and related techniques in soil plant studies on sustainable agriculture and environmental preservation jointly org. By the IAEA and the FAO and held in Vienna, 17-21 October 1999. Vienna, pp 597–619
- White RG, Kirkegaard JA (2010) The distribution and abundance of wheat roots in a dense, structured subsoil—implications for water uptake. *Plant Cell Environ* 33:133–148
- Yunusa IAM, Newton PJ (2003) Plants for amelioration of subsoil constraints and hydrological control. The primer-plant concept. *Plant Soil* 257:261–281
- Zarebanadkouki M, Ahmed MA, Carminati A (2016) Hydraulic conductivity of the root-soil interface of lupin in sandy soil after drying and rewetting. *Plant Soil* 398:267–280
- Zhu YG, Smolders E (2000) Plant uptake of radiocaesium: a review of mechanisms, regulation and application. *J Exp Bot* 51:1635–1645